Trees (2010) 24:931–940
DOI 10.1007/s00468-010-0464-3

ORIGINAL PAPER

Radial shrinkage and ultrasound acoustic emissions of fresh versus pre-dried Norway spruce sapwood

Sabine Rosner · Johannes Konnerth · Bernhard Plank · Dietmar Salaberger · Christian Hansmann

Received: 7 December 2009 / Revised: 17 June 2010 / Accepted: 24 June 2010 / Published online: 7 July 2010

Abstract Acoustic emission (AE) and radial shrinkage were compared between fully saturated fresh and pre-dried Norway spruce sapwood during dehydration at ambient temperature. Hydraulic conductivity measurements, anatomical investigations on bordered pits and X-ray computed tomography (CT) scans were done to search for possible AE sources other than the breakage of the water columns inside the tracheids. Both fresh and pre-dried specimens showed radial shrinkage due to drying surface layers right from the beginning of dehydration, which induced almost no AE. Whereas no dimensional changes occurred in pre-dried wood thereafter, fresh wood showed a rapid shrinkage increase starting at 25% relative water loss. This dimensional change ceased when further moisture got lost and was even partially reversed. AE of fresh wood showed much higher activity and energy, which is a waveform feature that describes the strength of the acoustic signal. Extremely high single AE energy events were detected at this critical stage of dehydration. After partial recovery from shrinkage, neither dimensional changes nor AE activity showed differences between fresh and pre-dried wood after more than 80% relative moisture loss. Our results suggested that fresh sapwood is more prone to dehydration stresses than pre-dried sapwood. Differences in AE and shrinkage behavior might be due to the weakening or distortion of the pit membranes (cavitation fatigue), pit aspiration, structural changes of the cell walls and micro-checks, which occurred during the first dehydration cycle.

Keywords Bordered pits · Cavitation fatigue · Functional wood anatomy · Hydraulic conductance · Norway spruce (*Picea abies*) · Acoustic emission testing · Wood shrinkage · X-ray computed tomography

Communicated by H. Cochard.

S. Rosner (✉)
Department of Integrative Biology, Institute of Botany, University of Natural Resources and Applied Life Sciences, BOKU Vienna, Gregor Mendel-Str. 33, 1180 Vienna, Austria
e-mail: sabine.rosner@boku.ac.at

J. Konnerth
Department of Material Sciences and Process Engineering, Institute of Wood Science, University of Natural Resources and Applied Life Sciences, BOKU Vienna, Gregor Mendel-Str. 33, 1180 Vienna, Austria

B. Plank · D. Salaberger
Upper Austria University of Applied Sciences, Stelzhamerstrasse 23, 4600 Wels, Austria

C. Hansmann
Competence Centre for Wood Composites and Wood Chemistry, St.-Peter-Str. 25, 4021 Linz, Austria

Introduction

In many conifer species, dehydration stress leads to a loss in mechanical strength in re-wetted wood due to structural changes of the tracheid walls and micro-cracks (Müller et al. 2004; Nair et al. 2009; Sakagami et al. 2007, 2009). In conduits that still contain free water, high negative pressures that develop during dehydration can induce a weakening or distortion of the pit membranes (Hacke et al. 2001; Sperry et al. 2003; Domec et al. 2006) or irreversible aspiration of the bordered pits (Liese and Bauch 1967; Greaves 1973; Domec et al. 2006). Permanent closure of bordered pits during heartwood formation minimizes the permeability of conifer wood (Hansmann et al. 2002) and might as well affect the shrinkage behavior. Heartwood, for

example, does not contribute to diameter changes of wood logs at moderate moisture loss (Irvine and Grace 1997).

Cell wall shrinkage is initiated when the moisture content of single tracheids drops below fiber saturation: that is, when the conduit contains no longer free water but the cell walls are fully saturated with liquid (Stamm 1971; Skaar 1988; Berry and Roderick 2005). The cellulose microfibrils of the tracheid walls are embedded in an amorphous matrix. When the matrix loses water, it tends to contract isotropically. In resisting this contraction, the microfibrils deform the matrix (Barber and Meylan 1964). Dimensional changes can however be observed long before most of the tracheids reach fiber saturation. Recently, we investigated the radial shrinkage behavior of fresh Norway spruce sapwood from full saturation till the cessation of shrinkage at ambient climatic conditions (Rosner et al. 2009). Dimensional changes induced by negative pressures of free water within the tracheids can be found already at moderate moisture losses (Irvine and Grace 1997; Perré 2007). Similar dimensional changes can be observed as diurnal stem diameter changes in living trees out in the field (Neher 1993; Herzog et al. 1996; Offenthaler et al. 2001; Perämäki et al. 2001; Zweifel et al. 2001; Ueda and Shibata 2001; Conejero et al. 2007). Negative hydrostatic pressures acting perpendicular to the cell walls try to draw the walls inward. When the negative pressure becomes too high, the water column will break leading to a sudden stress release (Tyree and Sperry 1989; Tyree and Zimmermann 2002). Shrinkage of fresh Norway spruce wood at moderate moisture loss was therefore found to be reversible to some extent (Rosner et al. 2009). This reversibility is not due to cell wall rewetting of the outer parts of the specimen by movement of free water from the inner wood parts, because wood moisture near the specimen surface of Norway spruce wood does not increase during a dehydration cycle (Tarmian et al. 2009). The dimensional change due to negative hydrostatic pressure is only partly reversible because it is masked by cell wall shrinkage during late dehydration stages, when the drier shell of the specimen reaches water contents below fiber saturation. After the shrinkage recovery peak, cell wall shrinkage is initiated when most of the tracheids reach fiber saturation (Rosner et al. 2009).

Drying checks develop because fiber saturation is reached far earlier in the shell than in the core of a specimen and because wood is an anisotropic material concerning cell wall shrinkage (Skaar 1988; Simpson and TenWolde 1999; Sakagami et al. 2009). Some authors suggest, however, that internal checking can be induced as well by the negative pressure of free water because checking occurs long before most cells reach fiber saturation (Quarles 1992; Booker 1994; Ball et al. 2005). Acoustic emission (AE) testing is a useful tool for optimizing lumber drying conditions, where the analysis of the amplitude or energy distribution of AE signals has been successfully used to pinpoint internal checking (Beall 2002; Kawamoto and Williams 2002; Beall et al. 2005). The bulk of ultrasonic AE (>15 kHz) during lumber drying is induced by the breakage of the water columns inside the tracheids due to high negative hydrostatic pressures (Tyree et al. 1984; Kawamoto and Williams 2002). The sudden stress release induces AE with the highest amplitudes in the range of 100–300 kHz (Sandford and Grace 1985; Tyree and Sperry 1989; Tyree and Zimmermann 2002). Crack formation during dehydration is indicated by a high AE burst rate and by AE signals with very high amplitudes or energies (Quarles 1992; Niemz et al. 1994; Cunderlik et al. 1996; Beall et al. 2005).

Combined shrinkage and AE tests from the fully saturated state to the end of shrinkage are scarce in literature (Rosner 2007; Rosner et al. 2009). In this study, we tested if pre-dried fully saturated Norway spruce sapwood shows the same dimensional changes during dehydration as never-dried fresh sapwood. Acoustic emissions feature analysis was used to detect periods of severe dehydration stress. Hydraulic conductivity measurements, anatomical investigations and X-ray computed tomography scans were done to relate possible differences in the shrinkage behavior to cavitation fatigue, defined as a weakening of the pit membrane for avoiding the breakage of the water columns, to aspiration of bordered pits and to mechanical failure.

Materials and methods

Preparation of standard beams

Wood specimens came from two 50-year-old healthy, dominating Norway spruce (*Picea abies* (L.) Karst.) harvested in Prinzersdorf (Lower Austria) in June 2008 and July 2009. Wood bole segments, 20 cm in length, were taken immediately after felling at 3–4 m height from the ground. During transport to the laboratory, the bole segments were kept wet in plastic bags containing some fresh water. Wood bole segments were debarked and split along the grain. Split samples from the tree harvested in July 2009 were stored frozen at −18°C until further preparation steps (Mayr et al. 2003, Rosner et al. 2006).

Outer sapwood specimens with a transverse surface of about 0.9 × 0.9 cm were isolated by splitting the wood along the grain with a chisel. Tangential and radial faces of the beams were planed on a sliding microtome. Specimens were shortened on a band saw, and sample ends were re-cut using a razor blade. During all these steps, the wood specimens were kept wet. Green wood specimens were then soaked in distilled water under vacuum for 24 h to

refill embolized tracheids (Hietz et al. 2008) and afterward stored at 4°C in degassed water containing 0.01 vol.% Micropur (Katadyn Products Inc., Switzerland) to prevent microbial growth. The final standard shape of the specimens was 0.6 cm tangential, 0.6 cm radial and 10.0 cm longitudinal in dimension.

AE and shrinkage testing

AE and shrinkage testing was performed on dehydrating fully soaked fresh sapwood specimens. After dehydration, pre-dried specimens were re-soaked in distilled water under vacuum for at least 96 h (Hietz et al. 2008) and a second round of AE and shrinkage testing was started when the specimen reached its former saturated weight. Fresh and pre-dried wood specimens were dehydrated for 24 h at ambient climatic conditions (25°C, 30% RH) to the equilibrium moisture content of 9.5 ± 0.2%.

AE (acoustic emission) was monitored with the μDiSP^{TM} Digital AE system from Physical Acoustics Corporation (Princeton Jct, PA, USA). Preamplifiers (40 dB) were used in connection with resonant 150 kHz R15C transducers with a standard frequency range of 50–200 kHz. Data were recorded with a detection threshold of 30 dB (0 dB = 1 μV input). The AE energy, also referred to as "energy counts", is dimensionless and calculated from the area of the rectified voltage signal over the duration of the AE signal.

AE transducers were positioned on the tangential face of fully saturated standard beams using an acrylic resin clamp, which is described in detail in Rosner et al. (2009). Silicone paste (Wacker, Burghausen, Germany) served as a coupling agent. The sample was positioned on a sample holder fixed on a compression spring. The compression spring below the sample holder was used to minimize the decrease in contact pressure during the wood shrinkage processes. Wood shrinkage was assessed by a load cell (DMS, Type 8416-5500, range 0–500 N; amplification with an inline amplifier for DMS, Type 9235; Burster, Gernsbach, Germany) between the AE transducer and the screw of the acrylic resin clamp. Contact pressure between transducer and wood was set to 30 N (Jackson and Grace 1996; Beall 2002) and the clamp assembly was kept so deep in water that the wood sample was totally covered till the applied pressure reached a constant value, which was achieved after less than 20 min, corresponding to observations by Cheng et al. (2004). After quickly removing superficial water from the assembly and the wood, recording of AE and coupling pressure was started. The clamp assemblage was positioned on a balance (resolution 10^{-3} g, Sartorius, Göttingen, Germany) and water loss was quantified automatically every 10 min. AE and shrinkage testing was done until the contact pressure reached a constant value, which took less than 24 h. Cumulated radial shrinkage (given in negative percent values) was calculated for 10-min time steps by relating the total radial shrinkage (digital gauge, accuracy 1 μm, Mitutoyo Corporation, Japan) to the total coupling pressure decrease (Rosner et al. 2009).

Dry weight (DW) of the wood beams was obtained by drying wood specimens after the second AE and shrinkage testing round at 103°C to constant weight to calculate the relative water loss (R). R (%) was calculated as: (1−(FW−DW)/(SW−DW)) × 100, where FW was the fresh weight at varying moisture content and SW the weight at full saturation. Radial shrinkage was referred to the nearest 5% R step. Analysis of contact pressure and AE data filtering was achieved with Vallen VisualAE^{TM} software (Vallen Systeme GMbH, Munich, Germany). AE signals that passed the detection threshold only twice were excluded from analysis (Rosner et al. 2009). A mean AE energy value was calculated for 10-min time steps. Cumulative AE and AE Energy were referred to the nearest 5% R step.

Hydraulic conductivity and vulnerability of fresh and pre-dried sapwood

Specific hydraulic conductivity was determined on saturated fresh and on saturated pre-dried standard wood beams by means of the modified Sperry apparatus designed by Mayr (2002) equipped with membrane-lined pressure sleeves (Spicer and Gartner 1998). Conductivity measurements were carried out under a hydraulic pressure head of 5.4 kPa with distilled, filtered (0.22 μm) and degassed water containing 0.005 vol.% Micropur. Specific hydraulic conductivity (k_s) is defined as:

$$k_s[\mathrm{m^2\ s^{-1}\ MPa^{-1}}] = Q \times l \times A_s^{-1} \times \Delta P^{-1},$$

where Q is the volume flow rate [$m^3\ s^{-1}$], l is the length of the segment [m], A_s is the sapwood cross-sectional area [m^2], and ΔP is the pressure difference between the two ends of the segment [MPa]. Conductivity data were corrected to 20°C to account for the temperature dependence of fluid viscosity.

Hydraulic vulnerability was tested on a parallel sample set of five fresh and five pre-dried re-saturated standard beams, which were produced from the Norway spruce tree harvested in 2009. Vulnerability curves for trunk wood were obtained with the method described in Domec and Gartner (2001). After determination of the saturated weight and the conductivity at full saturation, air overpressure was applied to the lateral sides of the specimens, while the transverse ends protruded from a double-ended pressure chamber (PMS Instruments Co., Corvallis, Oregon). After pressure treatment, the specimens were weighed and put in distilled water for 30 min. After re-cutting, the specimen hydraulic conductivity was measured again. Initially, the

pressure chamber was pressurized to 1 MPa, and the pressure was subsequently increased after each conductivity measurement in steps of 1 MPa until more than 90% loss of conductivity (PLC) was reached. Hydraulic vulnerability curves were fitted by cubic functions to calculate the pressure at which 50 PLC occurred. Dry weight was obtained by drying wood specimens at 103°C to constant weigh and R was calculated.

Anatomical investigations

Fully saturated fresh and pre-dried wood specimens were dehydrated in ethanol and embedded in Technovit 7100 (Heraeus Kulzer GmbH, Wehrheim, Germany). Semi-thin sections (1–3 μm) were made on a Reichert Jung Rotocut microtome (Modell 1165, Nußloch, Germany) using a Kulzer Histoknife H (Heraeus Kulzer GmbH, Wehrheim, Germany). Sections were stained with toluidine blue (Riedel-de Haen, Seelze, Germany) and mounted in Entellan (Merck, Darmstadt, Germany). Bordered pits were observed with a Leica DM4000M microscope equipped with a Leica DFC320 R2 digital camera and Leica IM 500 Image Manager image analyzing software (Leica, Wetzlar, Germany).

Scans of dried fresh samples by X-ray computed tomography

For the investigation of the dried fresh samples, a volume of about $7 \times 7 \times 7$ mm^3 was scanned by the nondestructive testing method of X-ray computed tomography (CT). The X-ray tomograms were scanned using a Nanotom 180NF CT device constructed by *GE* phoenix/X-ray (Wunstorf, Germany) with a 180 kV nano focus tube and a 2300×2300 pixel Hamamatsu detector (Hamamatsu City, Japan). The target used was made of molybdenum. The used resolution (voxel size) was 4.5 μm, the voltage at the nano focus tube was 55 kV, the measurement current 250 μA, the integration time at the detector 500 ms and the number of projections 1,700. These parameters lead to measurement time of about 100 min. CT data were reconstructed by using the Nanotom reconstruction software. Further artifact correction such as beam-hardening correction of the CT data or any kind of filter methods to reduce the noise was not applied.

The CT data were evaluated by the commercial software VGStudio Max v2.0 written by Volume Graphics GmbH (Heidelberg, Germany). For further evaluation of the CT data, image stacks (file format: TIFF) with a step size of 10 μm were exported. The images of such an image stack can be viewed with a simple image viewer integrated in nearly every operating systems of a PC.

Specimen number and statistics

AE feature extraction, shrinkage assessment and flow experiments were performed on nine mature fresh and refilled sapwood specimens, respectively. Hydraulic vulnerability was tested on five fresh and refilled sapwood beams, respectively. Anatomical investigations were done on a selected sample set of three fresh and refilled wood beams, respectively. CT scans were done on three air-dried fresh wood specimens. Statistical analysis was carried out with SPSS® 12.0. Values are given as mean ± standard error (SE). Mean values were tested for significance with the t test for independent samples, after analysis of variance and checking for normal distribution. Data sets with no normal distribution were tested for significant differences with the Mann–Whitney U test. Differences between mean values and relationships were accepted as significant if P was < 0.05.

Results

Dimensional changes and ultrasound acoustic emissions

Shrinkage experiments and AE testing were started in fresh and pre-dried wood at full saturation, which corresponded to 168.8 ± 1.3% moisture content. Both fresh and pre-dried specimens showed radial shrinkage due to drying surface layers right from the beginning of dehydration. This process induced almost no AE (Figs. 1, 2). In fresh wood, dimensional changes temporarily stabilized when the first AE was detected and reached thereafter a steeper slope at 24.5 ± 1.7% relative water loss (R). In pre-dried wood, radial dimension showed only a slight but continuous decrease (Fig. 2a). Maximum cumulated dimensional changes during this dehydration stage were two times higher in fresh than in pre-dried wood (1.26 ± 0.14%, 0.59 ± 0.05%, $P < 0.001$, Fig. 2a). In fresh dehydrating wood, very high single AE energies were measured at moderate water losses (Fig. 1a). Maximum AE energy/10 min was therefore much higher in fresh than in pre-dried wood (2.9 ± 0.2, 0.8 ± 0.1, $P < 0.0001$, Fig. 2c). Dimensional changes at moderate water losses were to 40.0 ± 6.8% reversible in both fresh and re-wetted wood (Fig. 2a).

Cell wall shrinkage started after the shrinkage recovery peak, in fresh wood at 73.9 ± 2.1% R and in pre-dried wood at 74.8 ± 2.4% R (Fig. 2a). Around the shrinkage recovery peak, single high energy AE events were detected in both fresh and pre-dried specimens. In fresh wood specimens, AE energies did not reach as high values as those detected at moderate moisture loss (Fig. 1a, b).

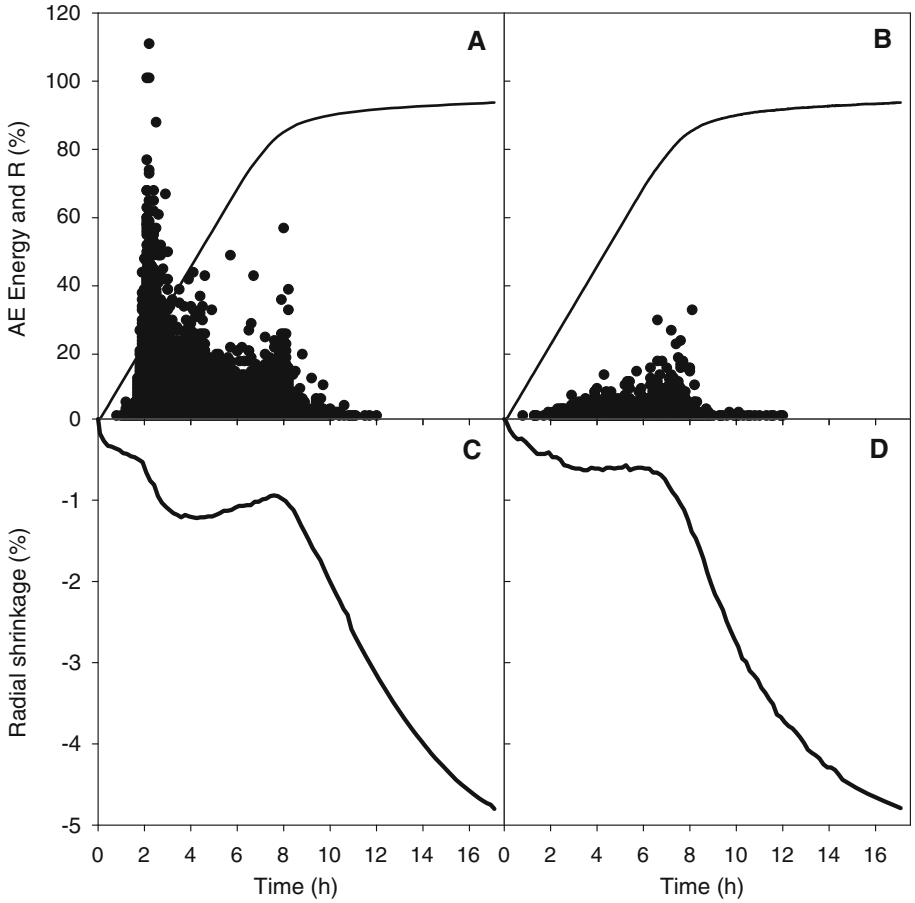

Fig. 1 Plots of single AE energy values (*dots*) and relative water loss (*line*) as well as the course of the radial dimensional changes against time of the same fresh (**a**, **c**) and pre-dried (**b**, **c**) dehydrating wood specimens

The total number of AE (numbers in 10^5 counts) was significantly higher in fresh than in pre-dried wood (4.1 ± 0.2, 2.1 ± 0.1, $P < 0.0001$, Fig. 2b).

Impact of drying on hydraulic vulnerability and conductivity

In pre-dried sapwood, the application of 2 MPa positive pressure resulted in a much higher relative release of water ($26.1 \pm 1.1\%$, $13.8 \pm 1.6\%$, $P < 0.001$, Fig. 3a) and loss of conductivity ($66.1 \pm 3.6\%$, $45.0 \pm 2.6\%$, $P < 0.01$, Fig. 3b) than in fresh sapwood. In pre-dried wood, much less positive pressure was therefore necessary to result in 50% loss of conductivity (1.5 ± 0.1 MPa, 2.0 ± 0.1 MPa, $P < 0.01$).

Bordered pits in the earlywood of fresh sapwood specimens were not aspirated. The pit membrane was positioned in the middle of the pit chamber allowing unrestricted water transport through the margo of the pit membrane (Fig. 4a–c). In pre-dried wood, however, a high number of bordered pits were found to be permanently aspirated. Especially in the first formed earlywood tracheids, the torus, which is the thickened middle part of the pit membrane, was pressed against the overarching pit border (Fig. 4d–e). Bordered pits in the later formed earlywood and latewood remained open; the pit membrane was located in the middle of the pit chamber (Fig. 4f). The tight sealing of the first formed earlywood tracheids should lead to an impairment of hydraulic conductivity. Accordingly, specific hydraulic conductivity was much higher in saturated fresh sapwood than in saturated pre-dried sapwood (24.0 ± 3.23 m^2 s^{-1} MPa^{-1} $\times$ 10^{-4}, 3.2 ± 0.6 m^2 s^{-1} MPa^{-1} $\times$ 10^{-4}, $P < 0.0001$).

Mechanical failure assessed by X-ray computed tomography (CT) scanning

An overview of a transverse CT scan is given in Fig. 5a. Light areas represent the dense latewood, darker regions less dense earlywood, and black areas air. We could not detect cracks with the resolution of 4.5 µm used for CT scanning. Radial resin canals might be misinterpreted as radial checks (Fig. 5b–d). When analyzing 10 µm CT stacks in the radial and tangential direction it however turned out that resin canals had a wider diameter at the transition zone between earlywood and the latewood formed in the previous year (Fig. 5b–d) and at locations with density variations (Fig. 5c).

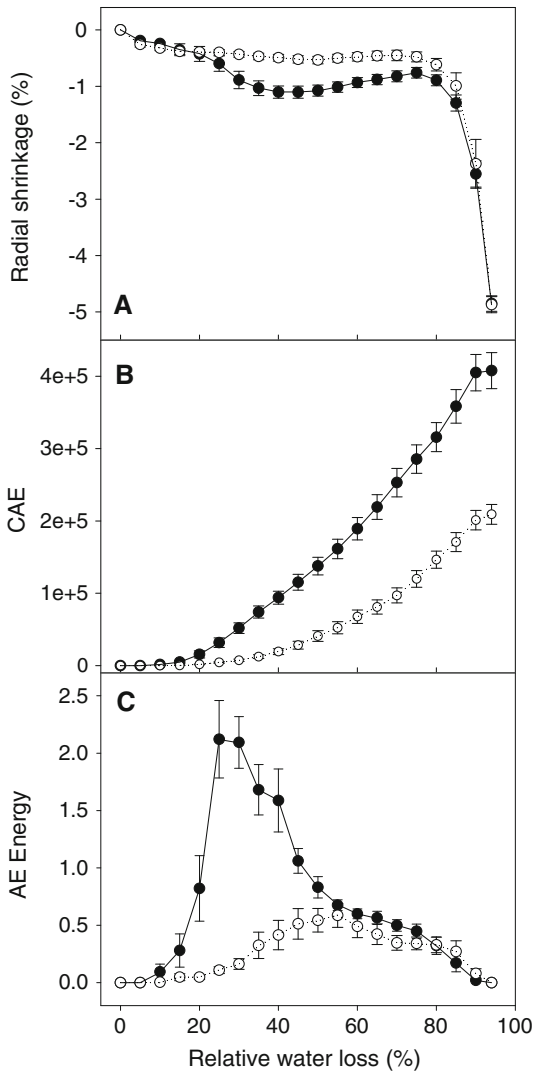

Fig. 2 Courses of radial dimensional changes (**a**), cumulative acoustic emission (**b**) and acoustic emission energy (**c**) in 5% relative water loss steps. *Error bars* show one standard error. *Filled symbols* and *solid lines* represent fresh wood; *empty symbols* and *dashed lines* represent pre-dried wood ($n = 9$, respectively)

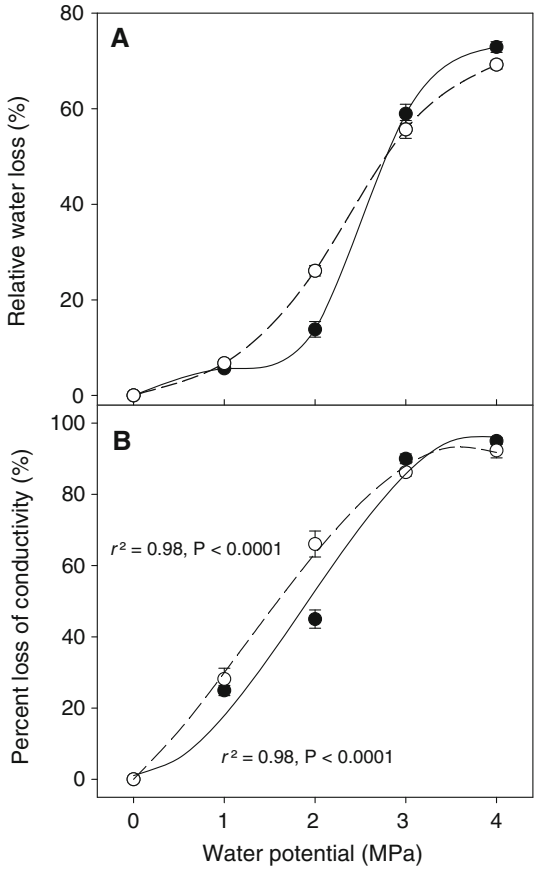

Fig. 3 Relative water loss (**a**) and percent loss of conductivity plotted against the application of positive pressure (**b**). *Error bars* show one standard error. *Filled symbols* and *solid lines* represent fresh wood; *empty symbols* and *dashed lines* represent pre-dried wood ($n = 5$, respectively). Hydraulic vulnerability curves were calculated from single measurements using cubic functions (**b**)

Discussion

Fresh sapwood was more prone to dehydration stress than pre-dried sapwood because we detected a lower number of AE with lower AE energies and measured a higher percentage of dimensional changes at moderate water losses. It is supposed that the dimensional change of fresh wood during early dehydration stages was merely induced by the negative pressure of free water inside the capillaries (Rosner et al. 2009). The negative pressure is released when it comes to the breakage of the water column (Irvine and Grace 1997; Offenthaler et al. 2001; Perré 2007). Fully saturated pre-dried wood showed a quite different behavior than fresh wood: the radial dimensions remained more stable till the initiation of the cell wall shrinkage process. Differences in AE and dimensional changes between fresh and pre-dried sapwood could have their causes in pit functioning and mechanical failure.

In spruce sapwood, earlywood pits of the first formed earlywood cell rows become irreversibly aspirated after dehydration, meaning that the pit membranes are permanently closed (Liese and Bauch 1967). The hydraulic conductivity at full saturation was therefore much lower in pre-dried than in fresh spruce wood. Conifer earlywood and latewood operate with different strategies of xylem safety for avoiding embolism. Whereas relatively mild drought stress leads to pit aspiration in earlywood tracheids, high tensions in latewood result rather in air seeding through pit membrane pores than in membrane closure of the pits (Gartner 1995; Hacke and Sperry 2001; Domec and Gartner 2002). If pit aspiration was a rapid process, it could be an AE source in fresh wood. Permanently closed pits in pre-dried wood will then produce no AE during the second dehydration cycle. Differences in the dimensional changes

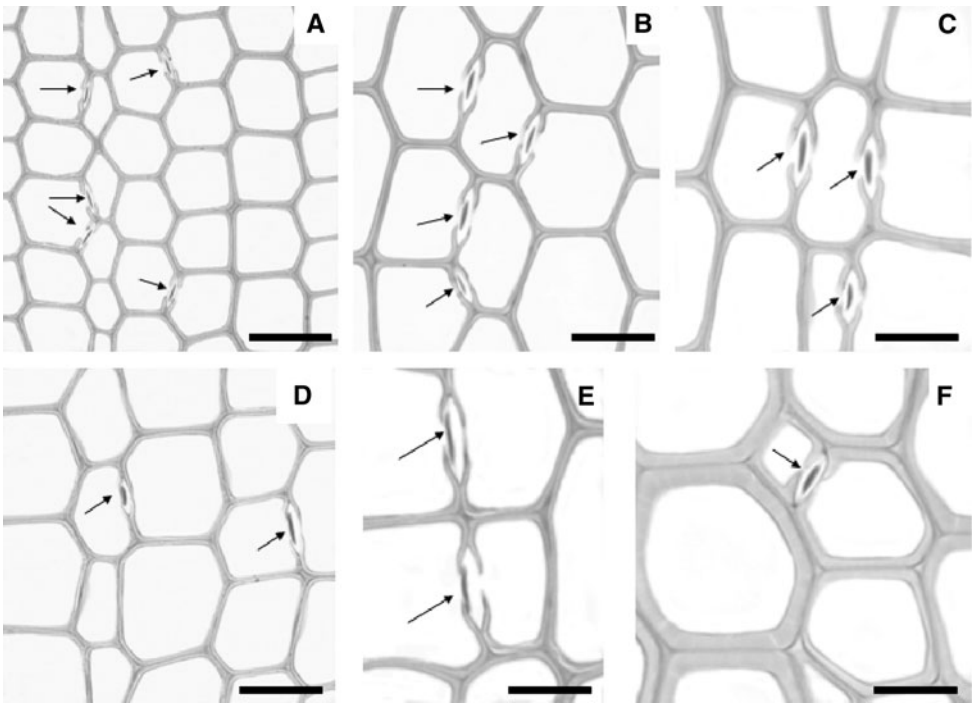

Fig. 4 Semi-thin transverse sections of fresh Norway spruce earlywood (**a**–**c**), pre-dried earlywood (**d**–**e**) and pre-dried wood from the earlywood–latewood transition zone (**f**). *Arrows* point at the darker stained torus of the pit membrane because toluidine blue stained the torus in dark lilac, which gave a strong contrast to the light blue-stained pit chamber walls and secondary cell walls of the tracheids. *Reference bars* represent 50 μm (**a**), 30 μm (**b**–**d**), 20 μm (**e**) and 10 μm (**f**)

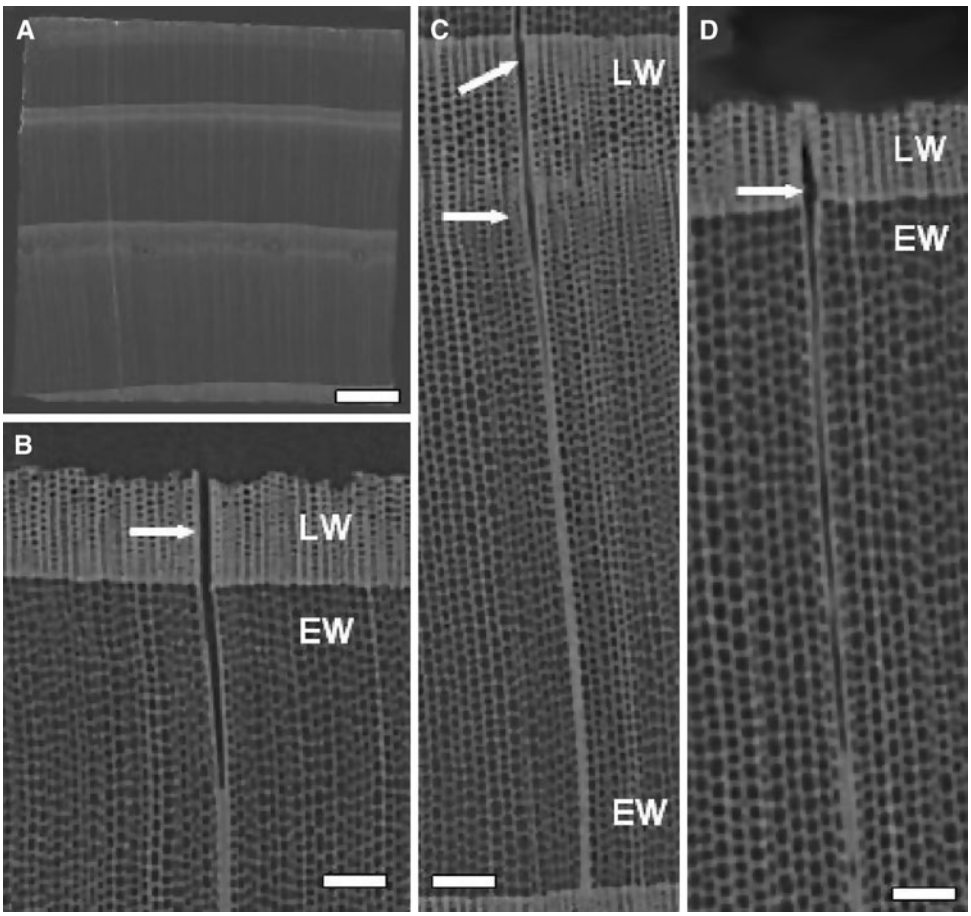

Fig. 5 X-ray CT scans of fresh dehydrated standard beams of Norway spruce. *Arrows* point at wood rays containing radial resin canals. *Reference bars* represent 1 mm (**a**), 200 μm (**b**, **c**) and 100 μm (**d**)

between fresh and pre-dried wood at moderate moisture loss might be partly explained by differences in the elastic stress response to negative pressure. Tensile stresses induced by negative pressures should be easier transmitted throughout free water in the wood via open earlywood pits. Pre-dried sapwood resembles somehow heartwood, where tracheids lose their function of water conductance due to pit aspiration (Hansmann et al. 2002). Heartwood does not contribute to the dimensional changes induced by negative pressures (Irvine and Grace 1997) probably because the conduits contain no or only a low amount of free storage water inside the conduits. But even if conduits would refill through the cell walls, pit aspiration might be advantageous for avoiding internal checking in living trees by reducing daily stem diameter variations. Booker (1994) supposed that sapwood within-ring internal checking was caused by water tension and not by differential shrinkage, because checking occurred long before most of the cells reached fiber saturation. Internal sapwood checks caused by negative pressure may also occur in living trees with low density earlywood during periods of summer drought and are a severe problem of short rotation forests (Rozenberg et al. 2002; Ball et al. 2005; Grabner et al. 2006).

Some pit membranes in earlywood pits can be also ripped out of their sealing position due to high negative water pressures (Hacke and Sperry 2001). An air injection pressure of 5 MPa can result in a broken torus of the pit membranes in Douglas fir earlywood (Domec et al. 2006). Pit membrane rupture processes caused by high negative pressures might be another AE source, which is present in fresh wood but not in pre-dried sapwood. It is not likely that such negative pressure is reached in mature spruce earlywood during dehydration because in the whole wood beam, almost 100% of hydraulic conductivity was already lost by application of 4 MPa pressure. Norway spruce trunk wood has however a much higher hydraulic vulnerability than Douglas fir trunk wood (Rosner et al. 2008; Domec et al. 2009). Therefore, much lower negative pressures might be necessary to cause pit membrane rupture in Norway spruce trunk wood.

Pre-dried wood was more vulnerable to the breakage of the water columns inside the tracheids than fresh wood: less pressure application was necessary in pre-dried than in fresh wood to result in 50% loss of hydraulic conductivity. Cavitation fatigue has been reported only for broadleaved species; there it is probably due to rupture or loosening of the cellulose mesh of inter-conduit pit membranes, which results in a weakened response of the pits to drought stress (Hacke et al. 2001; Sperry et al. 2003). Similar damage on the bordered pit membranes could lead also in conifer wood to a higher hydraulic vulnerability after refilling. But even if the pit membranes were not severed, after refilling small air bubbles might have been trapped in the conduits that could nucleate the breakage of the water columns prematurely during subsequent dehydration stress (Hacke et al. 2001). The lower deformation of water filled tracheids due to negative pressure associated with a lower total number of AE with weaker AE energies might be a direct function of the increased hydraulic vulnerability of pre-dried wood. Tracheids with bigger diameters and low wall/lumen ratio are more prone to deformation under negative pressure than tracheids with small diameters and high wall/lumen ratio before the breakage of the water column occurs (Rosner et al. 2009). If the water column breaks earlier in re-filled wood due to pit membrane weakening, the deformation induced by negative pressure will not reach the maximum value that is possible in fresh wood with intact pit membranes. If we assume an increase in hydraulic vulnerability for heartwood, cavitation fatigue might be somehow advantageous for minimizing dimensional changes induced by negative pressure.

During the first dehydration cycle, negative hydrostatic pressures or cell wall shrinkage might have as well induced micro-cracks. We could detect no mechanical failure with the resolution of 4.5 μm used for X-ray CT scanning. This however does not mean that mechanical failure did not occur, because in dried specimens it is sometimes hard to detect micro-cracks. Radial cracks associated with wood rays at the transition zone between earlywood and the latewood formed in the previous vegetation period close during the final stages of drying (Sakagami et al. 2009). High single AE events indicate mechanical failure in fresh wood at moderate water losses (Quarles 1992; Kawamoto and Williams 2002). Niemz et al. (1994) and Cunderlik et al. (1996) distinguished two stages during Norway spruce lumber drying by analyzing AE burst rates. The first peak in the AE rate was interpreted as checking caused by surface tension stress, and the second peak (at high water loss) as checking caused by tensile stresses inside the samples. The presence of small cracks could have caused lower stresses due to negative pressure during the second dehydration cycle after re-saturation.

Cell wall shrinkage after more than 80% relative water loss induced only a low number of AE with very low AE energies (Fig. 2). Attenuation in wood decreases, however, with increasing moisture loss (Beall 2002). Nevertheless, during the last stages of cell wall shrinkage, no AE was detected in both fresh and pre-dried wood (Fig. 1), which indicates that no mechanical failure occurred at high moisture losses (Booker 1994; Beall et al. 2005).

Conclusion

AE and shrinkage results suggested that fresh sapwood was more prone to dehydration stresses than pre-dried sapwood.

Differences in AE and shrinkage behavior might be due to changes in pit functioning and mechanical failure. Permanently closed pits, pit membrane rupture and micro-cracks that developed during the first dehydration cycle will produce no AE during the second dehydration cycle, after re-wetting. Additionally, cavitation fatigue might lower dehydration stress and thus dimensional changes because the breakage of the water columns occurs at less negative pressures. Therefore, a higher number of AE with higher AE energies were measured in fresh than in pre-dried dehydrating wood. If we assume that pre-dried wood resembles somehow heartwood, pit aspiration and cavitation fatigue might be advantageous for avoiding internal checking in living trees by reducing daily stem diameter variations.

Acknowledgments This study was financed by the Austrian Science Fund (FWF, Projects T304-B16 and V146-B16). We would like to thank the anonymous reviewer for helpful impact on the discussion of our results.

References

Ball RD, McConchie MS, Cown DJ (2005) Evidence for association between SilviScan-measured wood properties and intra-ring checking in a study of twenty-nine 6-year-old *Pinus radiata*. Can J For Res 35:1156–1172

Barber NF, Meylan BA (1964) The anisotropic shrinkage of wood. A theoretical model. Holzforschung 18:146–156

Beall FC (2002) Overview of the use of ultrasonic technologies in research on wood properties. Wood Sci Technol 36:197–212

Beall FC, Breiner TA, Wang J (2005) Closed-loop control of lumber drying based on acoustic emission peak amplitude. For Prod J 55:167–174

Berry SL, Roderick ML (2005) Plant–water relations and the fibre saturation point. New Phytol 168:25–38

Booker RE (1994) Internal checking and collapse—which comes first? In: Proceedings of the 4th IUFRO Wood Drying Conference: improving wood drying technology. Forest Research Institute, Rotura, pp 133–140

Cheng W, Morooka T, Liu Y, Norimoto M (2004) Shrinkage stress of wood drying under superheated steam above 100°C. Holzforschung 58:423–427

Conejero W, Alarcón JJ, Garcia-Orellana Y, Nicolas E (2007) Evaluation of sap and trunk diameter sensors for irrigation scheduling in early maturing peach trees. Tree Physiol 27:1753–1759

Cunderlik I, Molinski W, Raczkowski J (1996) The monitoring of drying cracks in the tension and opposite wood by acoustic emission and scanning electron microscopy methods. Holzforschung 50:258–262

Domec J-C, Gartner BL (2001) Cavitation and water storage in bole segments of mature and young Douglas-fir trees. Trees 15:204–214

Domec J-C, Gartner BL (2002) How do water transport and water storage differ in coniferous earlywood and latewood? J Exp Bot 53:2369–2379

Domec J-C, Lachenbruch B, Meinzer FC (2006) Bordered pit structure and function determine spatial patterns of air-seeding thresholds in xylem of Douglas-fir (*Pseudostuga menziesii*; *Pinaceae*) trees. Am J Bot 93:1588–1600

Domec J-C, Warren JM, Meinzer FC, Lachenbruch B (2009) Safety factors for xylem failure by implosion and air-seeding within roots, trunks and branches of young and old conifer trees. IAWA J 30:101–120

Gartner BL (1995) Patterns of xylem variation within a tree and their hydraulic and mechanical consequences. In: Gartner BL (ed) Plant stems: physiology and functional morphology. Academic Press, New York, pp 125–149

Grabner M, Cherubini P, Rozenberg P, Hannrup B (2006) Summer drought and low earlywood density induce intra-annual radial cracks in conifers. Scand J For Res 21:151–157

Greaves H (1973) Comparative morphology of selected sapwood species using the scanning electron microscope. Holzforschung 27:80–88

Hacke UG, Sperry JS (2001) Functional and ecological xylem anatomy. Perspect Plant Ecol Evol Syst 4:97–115

Hacke UG, Stiller V, Sperry JS, Pitterman J, McCulloh KA (2001) Cavitation fatigue. Embolism and refilling cycles can weaken the cavitation resistance of xylem. Plant Physiol 125:779–786

Hansmann C, Gindl W, Wimmer R, Teischinger A (2002) Permeability of wood—a review. Wood Res 47:1–16

Herzog KM, Häsler R, Thum R (1996) Diurnal changes in the radius of a subalpine Norway spruce stem: their relation to the sap flow and their use to estimate transpiration. Trees 10:94–101

Hietz P, Rosner S, Sorz J, Mayr S (2008) Comparison of methods to quantify loss of hydraulic conductivity in Norway spruce. Ann For Sci 65:5027

Irvine J, Grace J (1997) Continuous measurements of water tensions in the xylem of trees based on the elastic properties of wood. Planta 202:455–461

Jackson GE, Grace J (1996) Field measurements of xylem cavitation: are acoustic emissions useful? J Exp Bot 47:1643–1650

Kawamoto S, Williams RS (2002) Acoustic emission and acousto-ultrasonic techniques for wood and wood-based composites: a review. Gen Techn Rep FPL-GTR-134. U.S. Department of Agriculture, Forest Service, Forest Products Laboratory, Madison, pp 1–16

Liese W, Bauch J (1967) On the closure of bordered pits in conifers. Wood Sci Technol 1:1–13

Mayr S (2002) Eine modifizierte Sperry-Apparatur zur Messung des Emboliegrades im Xylem von Bäumen. Ber nat-med Verein Innsbruck 89:99–110

Mayr S, Rothart B, Dämon B (2003) Hydraulic efficiency and safety of leader shoots and twigs in Norway spruce growing at the alpine timberline. J Exp Bot 54:2563–2568

Müller U, Joscak T, Teischinger A (2004) Strength of dried and re-moistured spruce wood compared to native wood. Holz Roh- Werkstoff 61:439–443

Nair H, Butterfield B, Jackson S (2009) Are rays and resin canals sites for intra-ring checking in the wood of *Pinus radiata*? IAWA J 30:189–198

Neher V (1993) Effects of pressures inside Monterey pine trees. Trees 8:9–17

Niemz P, Emmler R, Pridöhl E, Fröhlich J, Lühmann A (1994) Vergleichende Untersuchungen zur Anwendung von piezoelektrischen und Schallemissionssignalen bei der Trocknung von Holz. Holz Roh- Werkstoff 52:162–168

Offenthaler I, Hietz P, Richter H (2001) Wood diameter indicates diurnal and long-term patterns of xylem water potential in Norway spruce. Trees 15:215–221

Perämäki M, Nikinmaa E, Sevanto S, Ilvesniemi H, Siivola E, Hari P, Vesala T (2001) Tree stem diameter variations and transpiration

in Scots pine: an analysis using a dynamic sap flow model. Tree Physiol 25:889–897

Perré P (2007) Experimental device for the accurate determination of wood–water relations on micro-samples. Holzforschung 61:419–429

Quarles SL (1992) Acoustic emission associated with oak during drying. Wood Fiber Sci 24:2–12

Rosner S (2007) Characteristics of acoustic emissions from dehydrating wood related to shrinkage processes. J Acoust Emiss 25:149–156

Rosner S, Klein A, Wimmer R, Karlsson B (2006) Extraction of features from ultrasound acoustic emissions: a tool to assess the hydraulic vulnerability of Norway spruce trunkwood? New Phytol 171:105–116

Rosner S, Klein A, Müller U, Karlsson B (2008) Tradeoffs between hydraulic and mechanical stress response of mature Norway spruce trunkwood. Tree Physiol 28:1179–1188

Rosner S, Karlsson B, Konnerth J, Hansmann C (2009) Shrinkage processes in standard-size Norway spruce wood specimens with different vulnerability to cavitation. Tree Physiol 29:1419–1431

Rozenberg P, Van Loo J, Hannrup B, Grabner M (2002) Clonal variation of wood density record of cambium reaction to water deficit in *Picea abies* (L.) Karst. Ann For Sci 59:533–540

Sakagami H, Matsamura J, Oda K (2007) Shrinkage of tracheid cells with desorption visualized by confocal laser scanning microscopy. IAWA J 28:29–37

Sakagami H, Tsuda K, Matsumura J, Oda K (2009) Microcracks occurring during drying visualized by confocal laser scanning microscopy. IAWA J 30:179–187

Sandford AP, Grace J (1985) The measurement and interpretation of ultrasound from woody stems. J Exp Bot 36:298–311

Simpson W, TenWolde A (1999) Physical properties and moisture relations of wood. In: Wood handbook-Wood as an engineering material. Gen. Techn. Rep. FLP-GTR-113. U.S. Department of Agriculture, Forest Service, Forest Products Laboratory, Madison, pp 3-1–3-24

Skaar C (1988) Wood–water relations. Springer, Berlin

Sperry JS, Stiller V, Hacke UG (2003) Xylem hydraulics and the soil–plant–atmosphere continuum: opportunities and unresolved issues. Agron J 95:1362–1370

Spicer R, Gartner BL (1998) Hydraulic properties of Douglas-fir (*Pseudotsuga menziesii*) branches and branch halves with references to compression wood. Tree Physiol 18:777–784

Stamm AJ (1971) Review of nine methods for determining the fiber saturation points of wood and wood products. Wood Sci 4:114–128

Tarmian A, Remond R, Faezipour M, Karimi A, Perré P (2009) Reaction wood drying kinetics: tension wood in *Fagus sylvatica* and compression wood in *Picea abies*. Wood Sci Technol 43:113–130

Tyree MT, Sperry JS (1989) Characterization and propagation of acoustic emission signals in woody plants: towards an improved acoustic emission counter. Plant Cell Environ 12:371–382

Tyree MT, Zimmermann MH (2002) Xylem structure and the ascent of sap. Springer, Berlin

Tyree MT, Dixon MA, Thompson RG (1984) Ultrasonic acoustic emissions from the sapwood of *Thuja occidentalis* measured inside a pressure bomb. Plant Physiol 74:1046–1049

Ueda M, Shibata E (2001) Diurnal changes in branch diameter as indicator of water status of Hinoki cypress *Chamaecyparis obtusa*. Trees 15:315–318

Zweifel R, Item H, Häsler R (2001) Link between diurnal stem radius changes and tree water relations. Tree Physiol 21:869–877